



RESEARCH ARTICLE

10.1002/2016EF000516

Far-field connectivity of the UK's four largest marine protected areas: Four of a kind?

J. Robinson^{1,2} , A. L. New¹, E. E. Popova¹ , M. A. Srokosz¹ , and A. Yool¹ ¹National Oceanography Centre, University of Southampton Waterfront Campus, Southampton, UK, ²Ocean and Earth Science, National Oceanography Centre Southampton, University of Southampton Waterfront Campus, Southampton, UK

Special Section:

Assessing Risk Governance Performance in the Face of Global Change

Key Points:

- Marine protected areas (MPAs), set up to protect endangered species, are vulnerable to upstream impacts from land due to ocean circulation
- Particle-tracking simulations show the land connectivity of four major British MPAs and give a “connectivity footprint” at annual timescales
- Connectivity to land differs substantially between MPAs with strong seasonal/inter-annual variability showing the utility of the footprints

Supporting Information:

- Supporting Information S1

Corresponding author:

A. Yool, axy@noc.ac.uk

Citation:

Robinson, J., A. L. New, E. E. Popova, M. A. Srokosz, and A. Yool (2017), Far-field connectivity of the UK's four largest marine protected areas: Four of a kind?, *Earth's Future*, 5, 475–494, doi:10.1002/2016EF000516.

Received 6 DEC 2016

Accepted 5 APR 2017

Accepted article online 13 APR 2017

Published online 17 MAY 2017

© 2017 The Authors.

This is an open access article under the terms of the Creative Commons Attribution License, which permits use, distribution and reproduction in any medium, provided the original work is properly cited.

Abstract Marine Protected Areas (MPAs) are established to conserve important ecosystems and protect marine species threatened in the wider ocean. However, even MPAs in remote areas are not wholly isolated from anthropogenic impacts. “Upstream” activities, possibly thousands of kilometers away, can influence MPAs through ocean currents that determine their connectivity. Persistent pollutants, such as plastics, can be transported from neighboring shelf regions to MPAs, or an ecosystem may be affected if larval dispersal is reduced from a seemingly remote upstream area. Thus, improved understanding of exactly where upstream is, and on what timescale it is connected, is important for protecting and monitoring MPAs. Here, we use a high-resolution (1/12°) ocean general circulation model and Lagrangian particle tracking to diagnose the connectivity of four of the UK's largest MPAs: Pitcairn; South Georgia and Sandwich Islands; Ascension; and the British Indian Ocean Territory (BIOT). We introduce the idea of a circulation “connectivity footprint”, by which MPAs are connected to upstream areas. Annual connectivity footprints were calculated for the four MPAs, taking into account seasonal and inter-annual variability. These footprints showed that, on annual timescales, Pitcairn was not connected with land, whereas there was increasing connectivity for waters reaching South Georgia, Ascension, and, especially, BIOT. BIOT also had a high degree of both seasonal and inter-annual variability, which drastically changed its footprint, year-to-year. We advocate that such connectivity footprints are an inherent property of all MPAs, and need to be considered when MPAs are first proposed or their viability as refuges evaluated.

Plain Language Summary Marine Protected Areas (MPAs) are typically established to conserve important ecosystems and protect marine species. However, even remote MPAs are not wholly isolated from impacts elsewhere, and can be connected via energetic ocean currents to impacts in “upstream areas” hundreds or even thousands of kilometres away. For instance, separate populations of marine species can be connected through larval dispersal by ocean currents, such that negative ecosystem impacts—overfishing or pollution—in a seemingly remote location may drastically affect a MPA. Here, we present “connectivity footprints” of four UK MPAs using a Lagrangian particle-tracking technique within a high-resolution ocean model, and evaluate their connectivity with land. At the 1-year timescale, Pitcairn is essentially unconnected with land, whereas the South Georgia, Ascension and BIOT MPAs are increasingly connected with remote land, with variability (seasonal and interannual) notably high for BIOT. In terms of exposure to pollution, we also consider the population density of connected coastlines, and identify this as an important risk factor in the management of MPAs. We advocate connectivity footprints of MPAs as a tool to improve future MPA designation, and in spatial planning of current MPA networks, and we suggest future work to better diagnose connectivity of MPAs.

1. Introduction

The world's oceans were once widely considered to be an inexhaustible resource, and consequently undervalued. However, it is now clear that the health of various ecosystems, and the fishery assets that they support, are deteriorating [Mills *et al.*, 2013; Doney *et al.*, 2014]. Global trends in world fisheries show a marked decline since the late 1980s, with over 500 species added to the Red List of Threatened Species of International Union for Conservation of Nature (IUCN)—the World Conservation Union [The World Bank, 2006; and references therein]. Consequently, food security issues are mounting with vulnerable communities in developing countries worst affected [Watson and Pauly, 2001; Pauly *et al.*, 2005; Golden *et al.*, 2016].

In response to this danger, and the mounting threat of climate change, new marine management and novel biodiversity conservation efforts are being developed and deployed worldwide in order to curb the negative trends [Halpern *et al.*, 2008; Day *et al.*, 2012; Barner *et al.*, 2015]. One such management tool is marine protected areas (MPAs), the definition of which varies considerably internationally, but a basic premise given by the IUCN describes “a clearly defined geographical space, recognized, dedicated and managed, through legal or other effective means, to achieve the long-term conservation of nature with associated ecosystem services and cultural values” [Dudley, 2008, p. 60]. The biodiversity, conservation, and fishery goals associated with MPAs are numerous and wide ranging, including habitat and biodiversity protection, ecosystem restoration, improved or restored fishery, the maintenance of spawning stock and spillover benefits into fishing grounds [Christie and White, 2007]. To validate the IUCN definition and realize these goals, it is necessary to minimize the impact of human activities on the MPAs, primarily achieved through designating “no-take zones” to either completely stop or sustainably manage fishing in the area [Edgar *et al.*, 2014].

An important component of the MPA framework is the areas' connectivity with its surroundings. In the marine environment, connectivity plays a much more important role than on land, as in the ocean everything is connected over long timescales [Jonsson and Watson, 2016]. Much work has gone into diagnosing biological outcomes of the downstream connectivity of MPAs, as it informs whether MPAs are successful in achieving conservation goals, such as seeding species in other areas, and also directs spatial management for further conservation efforts [Fogarty and Botsford, 2007; Christie *et al.*, 2010]. In order for sessile species to seed downstream, the timescale of connectivity is crucial, as the pelagic larval duration of the species obviously needs to be equal or greater than the connectivity timescale [Cowen *et al.*, 2007; Gawarkiewicz *et al.*, 2007]. However, both directions of connectivity are important, and one aspect of MPA connectivity, which has received relatively little research attention or policy consideration, is the possible negative impact of upstream connectivity. Upstream connectivity can determine an MPAs exposure to pollution, for instance it is a known issue that coastal MPAs, within close proximity to populated land, are at risk of pollution and other human impacts [Partelow *et al.*, 2015], but it is unclear whether these same risks apply to open sea MPAs as a consequence of oceanic circulation. Additionally, there could be an impact on the conservation efforts of the MPA if a key species in the ecosystem is being overfished upstream of the MPA [Stoner *et al.*, 2012], or risks from alien species which may become invasive as climate change forces species poleward [Wernberg *et al.*, 2011; Constable *et al.*, 2014].

In order to understand the upstream risks that an MPA is exposed to, and help MPAs achieve their conservation goals [Jameson *et al.*, 2002], it is necessary to diagnose the pathways of the water that flows into the region, and the timescales on which this occurs. In doing so, one needs to take into account seasonal and inter-annual variability of the ocean circulation. This study introduces the idea of a “connectivity footprint”, by which an MPA is connected to the upstream area via ocean currents, which can be estimated using high-resolution ocean circulation models. This paper examines the upstream connectivity of the UK's largest currently designated open seas MPAs, detailing the key circulation features and timescales in Section 3, then discusses an application of the concept of advective footprints to marine plastic which is considered to be the most significant and most widely spread form of marine pollution [Shahidul Islam and Tanaka, 2004; Gall and Thompson, 2015]. It should be noted, however, that with some minor modification of the experimental design, advective footprints can be applied to numerous other forms of marine pollution (e.g., oil spills or radioactive leaks), or to ecological impacts such as introduction of alien or invasive species by ocean currents.

In the first instance, we introduce the MPAs at the center of this study, followed by the methodology and experiment design.

1.1. Study Sites: Marine Protected Areas

In 2010, the United Nations set a target of protecting over 10% of the World Ocean by 2020 [Secretariat of the Convention on Biological Diversity, 2014]. Currently, however, only 2.8% is protected [International Union for Conservation of Nature (IUCN) and United Nations Environment Programme-World Conservation Monitoring Centre (UNEP-WCMC), 2013]. In view of this conservation target, in its 2015 manifesto the UK Conservative party promised to work toward preserving UK marine habitats, and outlined plans to create a “blue belt” of

Table 1. A Table of Basic Information on Each of the MPAs in This Study

	Pitcairn	S. Georgia	Ascension	BIOT ^a
Year designated	2015 ^b	2012	2016 ^c	2010
Location	24°S, 127°W	54°S, 36°W	7°S, 14°W	6°S, 71°E
SST ^d (°C)	24.75	1.78	25.89	28.19
MPA size (km ²)	834,334 ^e	1,070,000	234,291	545,000
No-take (%)	100	2	52.6 ^f	100
Island size (km ²)	62	3,755	88	60
Inhabitants ^g (#)	56	20	1,122	4,000
Threatened species ^h	37	9	53 ⁱ	81

BIOT, British Indian Ocean Territory; IUCN, International Union for Conservation of Nature; MPA, marine protected areas.

Information from [Petit and Prudent, 2010] and [Pelembé and Cooper, 2011], unless otherwise stated in the footnotes.

^aStatus currently under dispute, see Lunn [2016] for latest update.

^bOfficially designated, but not yet implemented [Alexander and Osborne, 2015].

^cOfficially designated, but not yet implemented [BLUE Marine Foundation, 2016].

^dSea surface temperature at the Lat/Lon given for each MPA, which is an average of six decadal climatologies (1955–2012) Locarnini et al. [2013].

^eThe Pew Charitable Trusts [2015].

^fCould be declared, subject to local agreement, as soon as 2017 [BLUE Marine Foundation, 2016].

^gIncludes temporary visitors at the time of census.

^hIUCN threatened species version 2015-4 *Animals* [The Red List, 2015].

ⁱNote that reported total threatened species for Ascension Island also include those of Saint Helena and Tristan da Cunha.

protected oceans around the UK's Overseas Territories [Alexander and Osborne, 2015]. Since then, it has designated an additional two new large MPAs in quick succession. However, monitoring these requires constant data-gathering and evaluation, in order to provide the best protection and conservation.

In this paper, we compare four of the largest, managed, marine British Overseas Territories: Pitcairn Island Marine Reserve (henceforth Pitcairn), South Georgia and South Sandwich Islands Marine Protected Area (South Georgia), Ascension Island Ocean Sanctuary (Ascension) and Chagos British Indian Ocean Territory Marine Protected Area (BIOT). For the purpose of this paper, we avoid the international ambiguity surrounding MPA terminology (*The World Bank*, 2006; see chapter 2) and will only consider the IUCN definition (Dudley, 2008, p. 60). We compare all four sites as equals, referring to them in text as MPAs, however, first we briefly introduce them here individually describing their current management as well as their general biomes and ecosystems.

Table 1 details some basic information about each of the MPAs included in this study, the locations of which can be seen in Figure 1, with the initial indicating each MPA. What is immediately apparent is the vast difference in size between the areas, with South Georgia being the largest and Ascension the smallest. In terms of threatened species, BIOT is the most precious habitat being home to over 80 IUCN Red List species [The Red List, 2015], however, all of the MPAs are important sanctuaries for threatened species.

Situated centrally in the South Pacific subtropics is the Pitcairn MPA, consisting of four remote islands which form part of the Polynesia/Micronesia biodiversity hotspot [Myers et al., 2000]. The Pitcairn Island is of volcanic origin, and is the only inhabited island of the four, whereas Henderson Island is a raised coral island, and the islands of Oeno and Ducie are small atolls. Currently, these coral reef communities are healthy environments, largely due to their uniquely isolated location and resulting near-pristine conditions [Friedlander et al., 2014]. In a bid to maintain the unspoilt nature of the Pitcairn Islands, the Exclusive Economic Zone (EEZ) surrounding Pitcairn has been designated as a marine reserve which will ban all commercial fishing in the area, but allow for the continuation of local fishing activities, once implemented. Due to the remote location of the islands, enforcing the ban will require satellite monitoring rather than the usual costly patrol

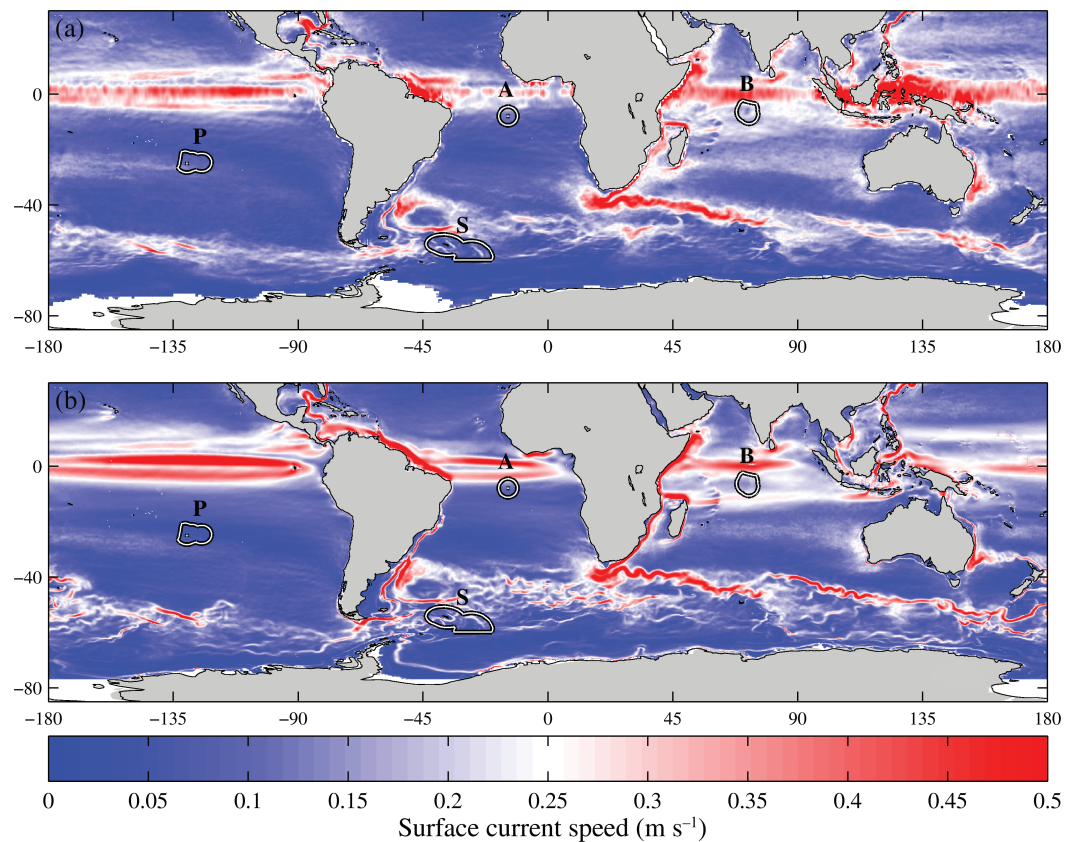


Figure 1. Observed and modeled decadal average, 2000–2009, surface current speed (m s^{-1}). The observed velocity, panel (a), is the Ocean Surface Current Analysis-Real-time data set at $1/3^\circ$ resolution and the modeled velocity, panel (b), is the Nucleus for European Modelling of the Ocean ocean general circulation model at $1/12^\circ$ resolution. The black and white contours denote the boundaries of the marine protected areas. The initials above each contour, represents: P for Pitcairn, S for South Georgia, A for Ascension, and B for British Indian Ocean Territory.

boats. Once an effective monitoring and enforcement regime is established and agreed upon by the Pitcairn community, interested non-governmental organisations (NGOs) and the UK government, the Pitcairn marine reserve will become one of the largest no-take areas in the world [Avagliano *et al.*, 2015].

Parts of the most productive waters of the Southern Ocean are found within the South Georgia MPA, located in the Atlantic sector, just east of Drake Passage. The MPA includes the South Sandwich Islands, which are approximately 700 km south-east of South Georgia. This diverse marine ecosystem is sustained by the nutrient-rich cold water, which upwells from the deep ocean, and supports an abundance of wildlife within its harsh polar environment [Murphy *et al.*, 2013]. Due to the nature of this inhospitable island, there are no permanent inhabitants, just temporary populations of government officials, scientists, and tourists. The islands are home to diverse communities of seabird species, a number of which are on the threatened species Red List [The Red List, 2015], and they are considered to be one of the most important seabird habitats in the world. Consequently, the MPA was designated in 2012, which prohibits all bottom trawling, a ban on bottom fishing at depths less than 700 m, and no-take zones (IUCN Category 1) around areas of high benthic biodiversity, totaling 20,431 km². Additionally, there are seasonal restrictions on certain fisheries to protect local predators [Petit and Prudent, 2010; Collins, 2013].

The most recently designated MPA in this study is the Ascension Island, which is situated just south of the equator in the Atlantic Ocean. Ascension Island is of volcanic origin and includes a few small uninhabited islands just offshore. The islands are young, formed only 1 million years ago, and consequently have relatively poor terrestrial biodiversity. However, due to its isolated location there are many endemic species, and the marine biodiversity is high. The island is also home to one of the most important populations of breeding Green turtles in the world, and is consequently considered to be an important habitat that needs

to be preserved [Pelembé and Cooper, 2011]. Ascension was designated as a marine reserve in 2016, closing just over half the reserve area to allow research to scope the eventual boundaries of the MPA, with the intention to assign the region a no-take area.

The BIOT MPA, also known as the Chagos Archipelago, is situated centrally within the Indian Ocean, half way between Africa and Indonesia and to the south of India. The area includes 55 coral islands spread over five atolls, of which Diego Garcia is the largest, with approximately 4,000 temporary residents. The 25,000 km² coral reefs of BIOT are unspoilt by human activity and in great health, owing to the protected status and the pristine waters, which could act as a global benchmark for unpolluted water [Guitart *et al.*, 2007]. This unique reef system supports a rich ecosystem that includes over 80 species on the threatened species list, and is consequently judged as possessing outstanding ecological value [Sheppard *et al.*, 2012]. In order to preserve this environment, in 2010 the UK government declared the area around BIOT as the then largest no-take marine reserve in the world at 544,000 km². Since that time, there have been legal issues surrounding BIOT's designation as an MPA. However, efforts are being made to confirm its status and ensure the future protection of this exceptionally well-preserved marine ecosystem [Lunn, 2016].

2. Methodology

In order to understand the potential exposure of MPAs to pollution and other risks, here we diagnose the connectivity to neighboring land masses through ocean circulation for each MPA. Once the connectivity is defined, it is then possible to assess the level of contact with human activity, and therefore risk. The tools and data used in this analysis are described here, along with the experimental design aimed at addressing these issues.

2.1. Ocean GCM and Lagrangian Particle Tracking

The Nucleus for European Modelling of the Ocean (NEMO) 1/12° resolution global ocean general circulation model (GCM) has been developed with particular emphasis on realistic representation of fine-scale circulation patterns [Marzocchi *et al.*, 2014], which provides an ideal platform to conduct Lagrangian particle-tracking experiments. Full details of the model run, including model setup and configuration, can be found in [Marzocchi *et al.*, 2014] so only a brief description will be given here. The model is initialized with World Ocean Atlas 2005 climatological fields and forced with realistic 6-hourly winds, daily heat fluxes, and monthly precipitation fields [Brodeau *et al.*, 2010]. The run begins in 1978, with output through to 2010, of which we are interested in 2000–2009. Model output is stored offline as successive 5 days means throughout the model run, of which the velocity fields are used for the particle tracking in this paper.

The Ariane package (<http://www.univ-brest.fr/lpo/ariane>) [Blanke and Raynaud, 1997] is applied to the NEMO velocity field to track 3D trajectories of water parcels using virtual particles that are released into the modeled ocean circulation [cf. Robinson *et al.*, 2014; Srokosz *et al.*, 2015; Popova *et al.*, 2016; who use a similar approach]. In our approach, the Lagrangian particles follow 3D velocity fields, and are not constrained to fixed release depths. Such an approach is most suitable to the dissolved marine pollutants, suspended type of plastic or larvae of marine organisms which have no or limited ability to control its vertical position. No diffusive processes were added to the transport of particles. These Lagrangian particles are intended here to represent water that enters within the boundaries of the MPAs. Further details about the Ariane package can be found in [Blanke and Raynaud, 1997; Blanke *et al.*, 1999].

The reader should note, however, that the Lagrangian approach used here is an approximation of online tracer release experiments. However, the latter are extremely computationally expensive both because they need to be performed in the full ocean model, and because each separate release experiments require its own separate tracer. The Lagrangian approach of offline approximation provides an alternative that allows large ensembles of computationally efficient experiments.

2.1.1. Modeled Versus Observed Surface Currents

The ability of the chosen model to accurately represent the circulation in the study areas is critical to the quality of the results. In order to qualitatively assess the performance of the NEMO 1/12° model, we compare the modeled surface velocity with the Ocean Surface Current Analysis-Real-time (OSCAR) dataset. The dataset provides global sea surface currents at 1/3° spatial resolution and a time resolution of 5-day

averages (available at <http://www.oscar.noaa.gov/>). The OSCAR velocity field is calculated by a linear combination of geostrophic, Ekman–Stommel, and thermal-wind currents [Johnson *et al.*, 2007]. OSCAR velocities provide accurate estimates of zonal and meridional time-mean circulation in comparison with the ship-board acoustic Doppler current profiler (ADCP) and drifter velocity estimates, although the product has weaker agreement with meridional currents in the near-equatorial region [Johnson *et al.*, 2007].

Figures 1a and 1b provide a comparison of the decadal (2000–2009) average ocean surface current speed, from OSCAR and NEMO, respectively, encompassing the four MPAs. The comparison shows good agreement between observed and modeled surface current speed, in terms of both the correct spatial pattern and magnitudes. The model does have known peculiarities at the equator, namely unexpected overturning cells at depth, however, this is unlikely to impact the surface or near-surface circulation. Additionally, the Antarctic Circumpolar Current, is known to be weaker in the model than the real world ocean, but the main circulation features of the Southern Ocean are in the correct location. There is also less small-scale variability in the model, owing to lower levels of eddy kinetic energy than the real ocean, despite the model being eddy-resolving at $1/12^\circ$ resolution. Nevertheless, studies have shown the model to realistically reproduce key circulation features, such as the North Atlantic Current and the Gulf Stream separation [Marzocchi *et al.*, 2014], and several western boundary currents [Popova *et al.*, 2016].

Figures S1–S4, Supporting Information, show the decadal, annual, and monthly averaged circulation, of both NEMO and OSCAR surface current speeds, around the region of each MPA for illustrative purposes.

2.2. Experiment Design

In order to diagnose the circulation pathways by which water reaches the four MPAs, Lagrangian particles were released at the start of each month into the modeled circulation, and followed backwards in time (backtracked) during January 2000 to December 2009. Consequently, each monthly release of particles is essentially the month in which the particles arrive at the MPA. Particle positions are recorded at 5-daily time intervals, for a total of 72 time-steps with 5-day intervals, an advection period of 1 year. For the purpose of this study, we found 1 year's worth of trajectories to be sufficient in assessing connectivity, as all but one MPA was connected to land within a 12-month period (details in Section 3). Nevertheless, we additionally performed 10-year duration sensitivity experiments to address the longer-term connectivity especially pertinent to the issues of plastic pollution (see Figures 3 and S5–S7). Particles are deployed at every fifth grid cell of the $1/12^\circ$ model grid horizontally (latitudinally and longitudinally) within the MPA boundaries, and at depths of 1, 20, 40, and 60 m to keep our approach generic and applicable to a wide range of problems. Figures S12 and S13 present a subsampling analysis that illustrates the low sensitivity of our analysis to the selected horizontal pattern of particle release. In case of plastics, such an approach would recognize both floating and suspended types, the latter being mostly spread over the well-mixed upper layer of the ocean. Particles were placed down to a depth of 60 m to approximate the euphotic zone (within which most planktonic organisms reside). The final boundaries of the Ascension MPA are not yet designated, so for the purpose of this study we have used the Ascension EEZ as the boundary. The particle placement was designed to be consistent in resolution across all MPAs for comparable analysis. However, the MPAs vary drastically in size (see Table 1), resulting in a different number of particles within each MPA experiment. At the horizontal and vertical grid spacing described, 1,888 Lagrangian particles are released at the beginning of each month for 10 years from the Pitcairn MPA, 6,155 particles from South Georgia MPA, 844 particles from the Ascension MPA, and 1,241 from the BIOT MPA.

2.3. Population Density Data

In discussing the MPAs connectivity with land in Section 3, exposure to risk is discussed in terms of connectivity with highly populated areas in Section 4. The population density data used for this is the Gridded Population of the World, Version 3 (GPWv3) Future Estimates for 2015 produced by [Center for International Earth Science Information Network, Columbia University United Nations, Food Agriculture Programme, and Centro Internacional de Agricultura Tropical, 2005], and can be seen in Figure 2. The GPWv3 dataset provides estimated population density in persons per square km at $1/4^\circ$ resolution across the globe. More information, as well as the dataset itself, is available at: <http://sedac.ciesin.columbia.edu/data/set/gpw-v3-population-density-future-estimates>.

As a first-order approximation of population density effects, the $1/4^\circ$ gridded population density field was extrapolated out from the land into the ocean, using the Matlab v2013a scatteredInterpolant function and

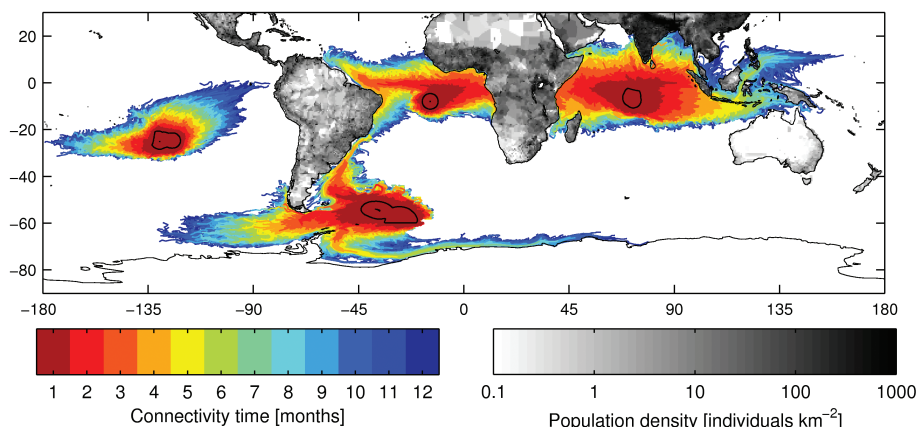


Figure 2. The time, in months, that it takes for ocean surface waters to reach the marine protected areas. The colored area represents the trajectories of particles, which arrive at the marine protected areas, each month during 2000–2009. The color of the trajectories indicate the time in months for the particles to be advected to the marine protected area, termed on the color bar as the connectivity time. The black contours represent the boundaries of the marine protected areas. The grayscale land indicates the population density, in persons per km² at 1/4° resolution. Note that trajectories representing shorter connectivity times are plotted after those representing longer times so that it is clear what the shortest connection time of a particular location to an marine protected areas.

natural neighbor interpolation. This approach does not factor in the effect of inland population density, i.e., where a stretch of coastline may be impacted by a significant inland population. However, restrictions in the availability of data mean that the GPWv3 dataset frequently averages population over an extended area, decreasing the significance of such errors (albeit locally). Note that this analysis also uses human population density as a proxy for impact, when the latter may actually be a stronger function of local technology, environmental regulations, and resource management.

The extrapolated population density was recorded for Lagrangian particle trajectories, which were within 85 km of the coastline. This distance is the global average width of the continental shelf [Elrod *et al.*, 2004], and we use such a fixed boundary to avoid biases introduced by the highly varying width of the continental shelf around the globe. Within this near-coastal zone, the water is considered as well-mixed [Nash *et al.*, 2012], and references therein), and, consequently, we assume water properties or human pollution, are evenly distributed throughout the shelf water mass.

3. Results

In order to assess the degree of exposure to pollution risk from upstream sources, we diagnose the pathways of the water that enters the MPAs and the associated timescales. Across parts of the World's Oceans, the circulation can shift both seasonally and inter-annually, and at varying magnitudes, which can significantly alter an MPA's connectivity. In this section, we describe the general circulation around the four MPAs, and the connectivity timescales with land. We then address the seasonal and inter-annual variability of the circulation, across a 10-year period.

3.1. General Circulation and Connectivity of MPAs

Figure 2 includes all of the particle data, across all months and years, in the experiments. Dark red trajectories represent an advection time of 1 month, before reaching the MPAs and consequently are the closest to the boundaries (black contours). Dark blue trajectories represent an advection time of 12 months, and are therefore at a greater distance from the MPAs. This figure illustrates the dominant pathways to the MPAs throughout a 10-year period, including inter-annual and seasonal variability.

What is apparent from Figure 2, is that all the MPA's, except Pitcairn, are connected with land within a 1 year timescale. As can be seen from Figure 1, the Pitcairn marine reserve is in an area of relatively slow surface currents. This is due to it being positioned toward the center of the basin-wide, anti-cyclonic South Pacific Gyre [Maes *et al.*, 2016]. There are two lobes of source water into the Pitcairn reserve, the main pathway originates in the northeast, and the second originates in the west. To further understand the circulation pattern around Pitcairn, a 10-year back tracking simulation was performed in order to identify the key circulation

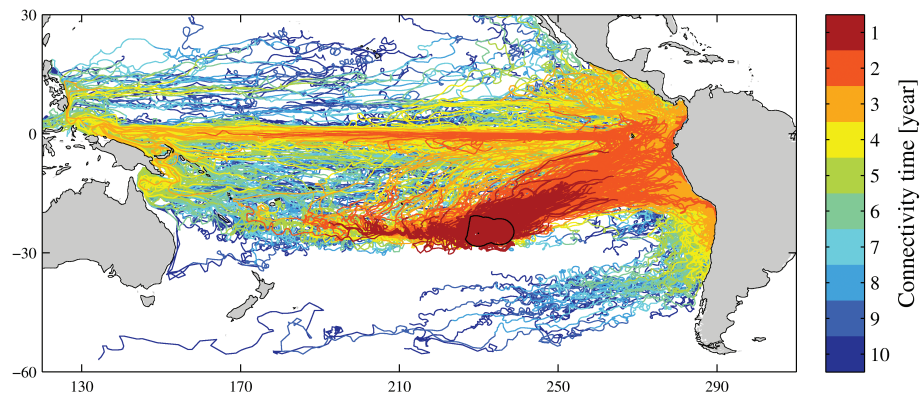


Figure 3. The time, in years, that it takes for ocean surface waters to reach the Pitcairn marine protected area. The colored area represents the trajectories of particles, which arrive at Pitcairn, each year during 2000–2009. The color of the trajectories indicate the time in years for the particles to be advected to the marine protected area, termed on the color bar as the connectivity time. The black contour represents the boundary of the Pitcairn marine protected areas. Note that trajectories representing shorter connectivity times are plotted after those representing longer times so that it is clear what the shortest connection time of a particular location to an marine protected areas.

features that influence the Pitcairn MPA (Figure 3). This revealed that two major currents feed the Pitcairn MPA, namely the Pacific Equatorial Undercurrent and the Humboldt Current. Particles traveling in the undercurrent across the entire basin, are at roughly 200 m on the western side, and gradually shoal as they travel toward the east [Grenier *et al.*, 2011]. Once reaching the west coast of South America, wind-driven coastal upwelling brings all particles to the surface [Talley *et al.*, 2011] eventually feeding into the Pitcairn surface waters by the circulation of the gyre. The Humboldt Current is an eastern boundary current flowing northwards along the west coast of the South American continent [Fiedler and Talley, 2006]. The northeastern lobe of the dominant pathway flows from the northwest coast of South America, whereas the western pathway is formed of water that has spent more time circulating in the anti-clockwise current of the sub-tropical gyre. Ekman transport causes the surface water to move toward the central region of a subtropical gyre [Eriksen *et al.*, 2013]. In terms of Pitcairn's connectivity, the MPA is connected to the South American continent within a 2-year timescale (via the northern arm of the South Pacific Gyre), and also the Malay Archipelago within 3–4 years (via the Pacific Equatorial Undercurrent). The longer-term (multiannual) connectivity described above for the Pitcairn MPA is important when the concept of circulation pathways is applied to issues such as plastic pollution, as marine plastic may degrade slowly [but see van Sebille *et al.*, 2015]. The corresponding long-term (10-year) connectivities of the other three MPAs are shown in Figures S5–S7.

The South Georgia MPA is fed by three dominant pathways: the Antarctic Circumpolar Current flowing from west to east around Antarctica; a southern pathway from the Antarctic Slope Current, with flows east to west along the Antarctic shelf [Rintoul *et al.*, 2001]; and a northern pathway via the return flow of the Malvinas Current, and also small but frequent eddies which are shed from the Brazil Current and are associated with the Subantarctic Front [Peterson and Stramma, 1991]. From these pathways, we can see in Figure 2 that the South Georgia MPA has a connectivity timescale in the order of 3–4 months. However, in considering the exposure to human activity, the only pathway for the South Georgia MPA that could be significant, taking into account population density, is from the Brazil Western Boundary Current, which flows southward along the east coast of the South American continent.

The Ascension MPA is positioned just south of the equator in the mid-Atlantic. Consequently, it is fed by two main pathways of water, the westward flowing South Equatorial Current and the eastward flowing North Equatorial Countercurrent. There is also an eastward flowing pathway, just sub-surface, via the Atlantic Equatorial Undercurrent [Brandt *et al.*, 2014]. The dominant pathway of water to the Ascension MPA is from the eastern side of the Atlantic, as seen in Figure 2. Parallel to the west coast of Africa, are two main currents each flowing in a meridional direction, which meet in a confluence region at about 15°S before turning west to become part of the South Equatorial Current. Flowing north to south is the Guinea Current and its extension the Angola Current, and flowing south to north is the Benguela Coastal Current [Lass *et al.*, 2000]. The highly seasonal eastward flowing North Equatorial Countercurrent originates from the western side of the

Atlantic at roughly 5–10°N [Richardson *et al.*, 1992]. A small proportion of the North Equatorial Countercurrent is fed by the northward flowing North Brazil Current, but the majority of the countercurrent is fed by northern hemisphere waters originating in the North Equatorial Current at roughly 10°N [Goes *et al.*, 2005]. The eastward flowing North Equatorial Countercurrent is strongest in the late boreal summer into fall, with a reversal of the near-surface current in spring due to a change in the Northeast Trade winds [Richardson *et al.*, 1992]. The Atlantic Equatorial current system connects the Ascension MPA with the west coast of Africa within a time period of 2–3 months, and with the east coast of Brazil within 3–4 months.

The BIOT MPA is positioned toward the center of the Indian Ocean, just south of the equator. In Figure 2, it is apparent that the BIOT MPA is fed by various water pathways from across the entire Indian Ocean, and also from the Pacific through the Indonesia Throughflow. The circulation of the Indian Ocean is extremely complex [Wyrtki, 1973], owing in part to the geographical configuration, but primarily to the unique monsoonal wind forcing. Here, we provide a brief description of the typical surface ocean circulation from the literature, focusing on key features relevant to the analysis.

The Indian Ocean is the smallest of the three major ocean basins, extending only as far north as 25°N on either side of the Indian subcontinent. The southern sector of the Indian Ocean is bounded by the Antarctic Circumpolar Current through which it is connected with the Atlantic and Pacific Oceans. There is also an important connection with the low latitude Pacific via the Indonesian Throughflow, which flows unidirectionally from the Pacific into the Indian through the Indonesian Archipelago. Once exiting the Archipelago, it flows westward within the South Equatorial Current. However, annual variability is high, and an El Niño/Southern Oscillation (ENSO) signal has been observed [Sprintall *et al.*, 2014]. In the southern half of the Indian Ocean is a basin-wide subtropical gyre, which flows anti-cyclonically driven by westerly winds at high (Southern) latitudes and south-easterly trade winds at low latitudes, similar to the mean wind patterns of the Atlantic and Pacific. The South Equatorial Current flows westward across the basin throughout the year at roughly 10–16°S, with a transport of some 50–55 Sv, and separates the subtropical south from the tropical and northern Indian Ocean [New *et al.*, 2007]. For parts of the year, a confluence of two currents at roughly 2–3°S along the east coast of Africa, results in the eastward flowing South Equatorial Countercurrent, which together with the South Equatorial Current, becomes the northern and southern branches of a transitory tropical cyclonic gyre [Schott and McCreary, 2001; Talley *et al.*, 2011].

North of the South Equatorial Current, is a unique circulation regime, which seasonally reverses driven by monsoonal wind forcing. The Southwest Monsoon winds peaks in July–August, and the Northeast Monsoon winds in January–February, driving seasonal reversals in the ocean currents in this region [Schott and McCreary, 2001]. Greatly influenced by the reversing Southwest and Northeast Monsoons, are the two large embayments to the east and west of the Indian subcontinent, the Arabian Sea and the Bay of Bengal, respectively. During the Southwest Monsoon (winds blowing to the north-east over India) the open-ocean currents that circulate between the Arabian Sea and the Bay of Bengal flow eastward (Southwest Monsoon Current), whereas flow is westward during the Northeast Monsoon (Northeast Monsoon Current), influencing the formation of the South Equatorial Countercurrent. These monsoon currents are made up of many different branches, each forced individually by a combination of both local and remote processes. However, the Northeast Monsoon Current is notably weaker and more disorganized than the Southwest Monsoon Current, as the Southwest Monsoon winds are stronger than the Northeast Monsoon winds. Consequently, the ocean response is stronger and more consistent to the Southwest Monsoon. The transition between Southwest to Northeast Monsoons, and vice versa, occurs relatively quickly during March–April and October, during which the equatorial winds are westerlies, rather than the typical trade winds [Schott and McCreary, 2001; Shankar *et al.*, 2002; Talley *et al.*, 2011]. This brief dominance of westerlies forms the eastward flowing Wyrtki Jets, which are significantly stronger than the westward flowing South Equatorial Current during this time [Wyrtki, 1973].

For a schematic diagram of the Indian Ocean circulation and a thorough description of the entire regime, see [Schott and McCreary, 2001; Figures 8 and 9]. For a more in-depth discussion specifically of the northern Indian Ocean monsoonal circulation, see [Shankar *et al.*, 2002].

In terms of connectivity timescales, the BIOT MPA is connected to: the east coast of Africa within 3 months advection time; to Indonesia within 3–4 months, and via the Indonesian Throughflow, to the Malay Archipelago within 4–7 months; and to India within a range of 3–6 months. Northwards of 20°S, particle

trajectories from the BIOT MPA fill the entire Indian Ocean basin, with the exception of the northern Arabian Sea.

Similarly to Figure 3's Pitcairn pathways, Figures S5–S7 show the decadal-scale connectivity for the South Georgia, Ascension and BIOT MPAs. In the case of the South Georgia MPA, its proximity to the Antarctic Circumpolar Current means that the entire Southern Ocean is connected to the MPA within a time period of around 5 years. However, in spite of this fast connectivity, pathways remain constrained within the Southern Ocean even out to 10 years—with a few exceptions in continental boundary currents. For the Ascension MPA, most connectivity is confined to the equatorial region of the Atlantic (30°S to 10°N) on the 5-year timescale. Beyond this, some pathways extend further, notably via Agulhas Leakage from the Indian Ocean (with limited connectivity to the Indonesian Throughflow), though also with pathways from the subtropical gyres of the north and, especially, south Atlantic. Finally, for the BIOT MPA, most pathways remain within, and completely fill, the Indian Ocean, with connectivity of 4 years or less throughout this basin. There is also connectivity with the equatorial Pacific (20°S to 20°N) through the Indonesian Throughflow, with a few pathways almost connecting to the west coast of the Americas at the 10-year timescale.

3.2. Seasonal and Inter-Annual Variability

Figure 4 shows all the particles from the monthly releases for each year of the experiment, indicating the density of the trajectories and the inter-annual variability for each MPA. For comparison, Figures S9–S11 show corresponding trajectory densities for shorter time periods.

Focusing on Pitcairn in Figure 4, the trajectory density “footprint” in each subplot is generally the same in each year with the two distinct lobes to the northeast and west. In some years, the particles backtrack further away from Pitcairn, such as in years 2006 and 2007, and in others the particles remain closer to the MPA boundary, such as in years 2002 and 2003. However, these variations are not large enough for any significant connectivity to any coastline.

For the South Georgia MPA, the highest trajectory density is within the Antarctic Circumpolar Current, indicating this to be the dominant pathway. Conversely, Figure 4 also shows that the lowest density of trajectories advecting toward the South Georgia MPA comes from the northern pathway. As with Pitcairn, the South Georgia MPA has little inter-annual variability.

Focussing next on the Ascension MPA, Figure 4 shows the dominant pathway of water to originate from the west coast of Africa, specifically the Benguela Current and South Equatorial Current, showing low inter-annual variability.

Finally, focusing on the BIOT MPA in Figure 4, there are two dominant pathways of surface water for the MPA, one each from the east and the west. However, there is a high degree of variability both across and within the years. In 2009, the dominant pathway is from the west, indicated by the logarithmic color bar. Whereas in 2003, the highest trajectory density is from the east, and in some years there are equally pronounced pathways from both the east and west. This variability has a significant impact on the connectivity of the BIOT MPA to various continents. The BIOT MPA experiences by far the highest degree of inter-annual circulation variability out of the four MPAs in this study.

In order to examine the seasonal variability of circulation around the BIOT MPA, Figure 5 shows the pathways for each climatological month that arrives at BIOT, from which the impact of the seasonally reversing circulation is apparent. Figure 5 shows that the key features that determine the dominant pathways to the BIOT MPA are the South Equatorial Current (including the Indonesian Throughflow), the periodic Countercurrent and Wyrki Jets, and the reversing Monsoonal Currents.

Focusing on one of the clearer features within Figure 5, it is apparent that the Indonesian Throughflow is an important pathway to the BIOT MPA of water arriving during September–December. Meyers *et al.* [1995], found that flow through the Indonesian Archipelago is largest during the Boreal summer, and taking into account an appropriate time lag between water passing through the Archipelago and arriving at BIOT, agrees with Figure 5 where there is a high density of particles within the Indonesian Throughflow during September–December arrival months. Other than the Indonesian Throughflow, the remaining picture is unclear, due to the reversal of the northern circulation and periodic appearance of the South Equatorial Countercurrent and Wyrki Jets.

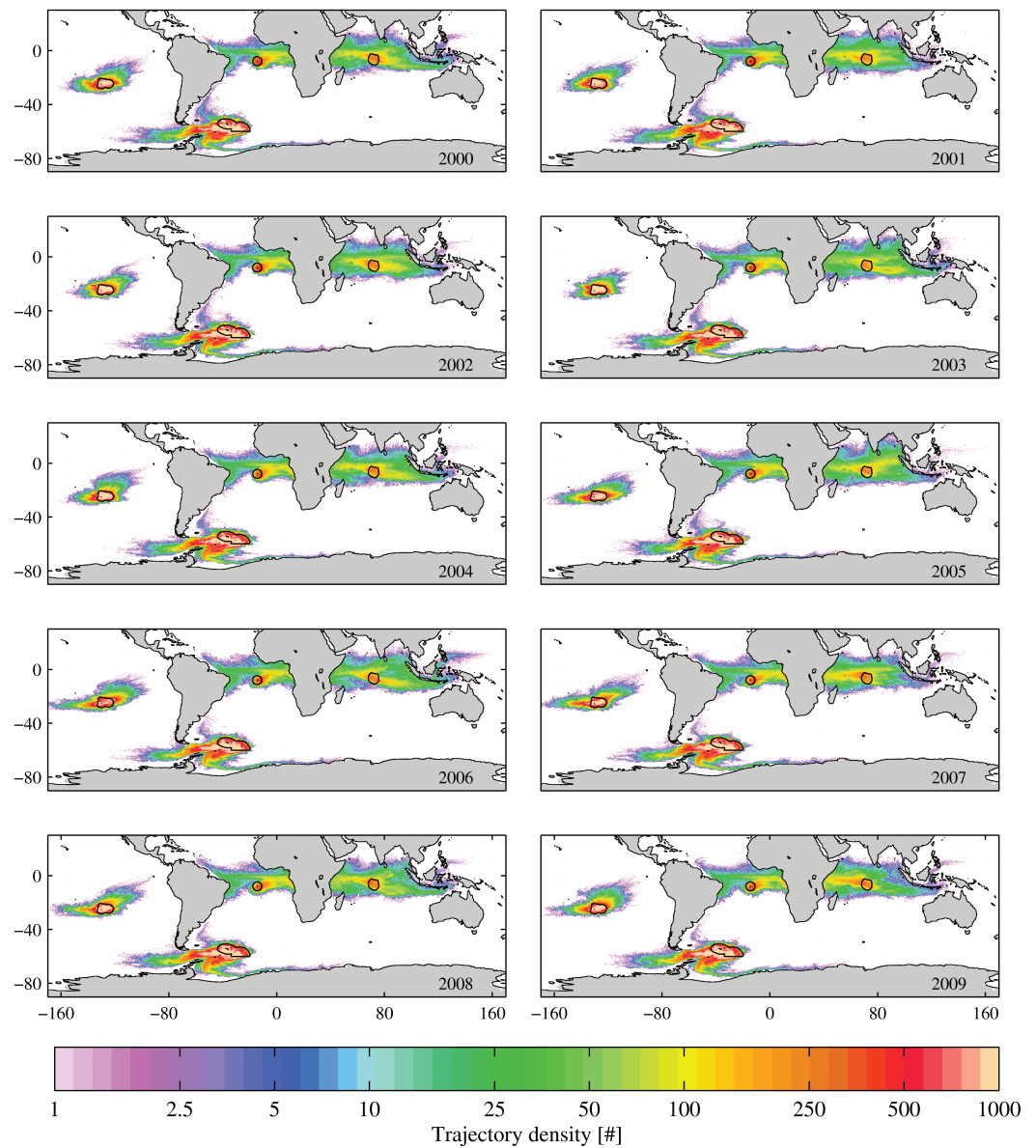


Figure 4. Census of particle advection toward the marine protected areas for each year's trajectories. The annual plots include all the particles released monthly from the marine protected area, each with an advection time of 1 year. Colors denote the cumulative "density" of particle trajectories based on their 5-daily position throughout the 10-year experiment, representing the total number of trajectories that have passed through each grid cell.

The complex, seasonally transforming, circulation pattern of the Indian Ocean is neither spatially nor temporally consistent year-on-year [Shankar et al., 2002; Schott et al., 2009]. This explains why Figure 5 does not clearly represent the monsoon driven circulation presented in Indian Ocean schematic circulation plots [such as Schott and McCreary, 2001; Figures 8 and 9]. As Figure 5 represents climatological months, the inter-annual variability smooths out the presence of any distinct features visible in the trajectories. To provide a clearer example, and also to demonstrate the degree of inter-annual variability in addition to the seasonal variability, Figure 6 shows four individual experiments of particle releases, arriving at the BIOT MPA within January and July, from a selection of years within the 10-year study period. Focusing on the top two panels, the predominant pathway arriving in January 2005 was from the northeast, the Bay of Bengal and Indonesia region, whereas in January 2009 the majority came from the western side of the basin. This inter-annual variability also occurs at other times of the year, as shown by the bottom two panels of water

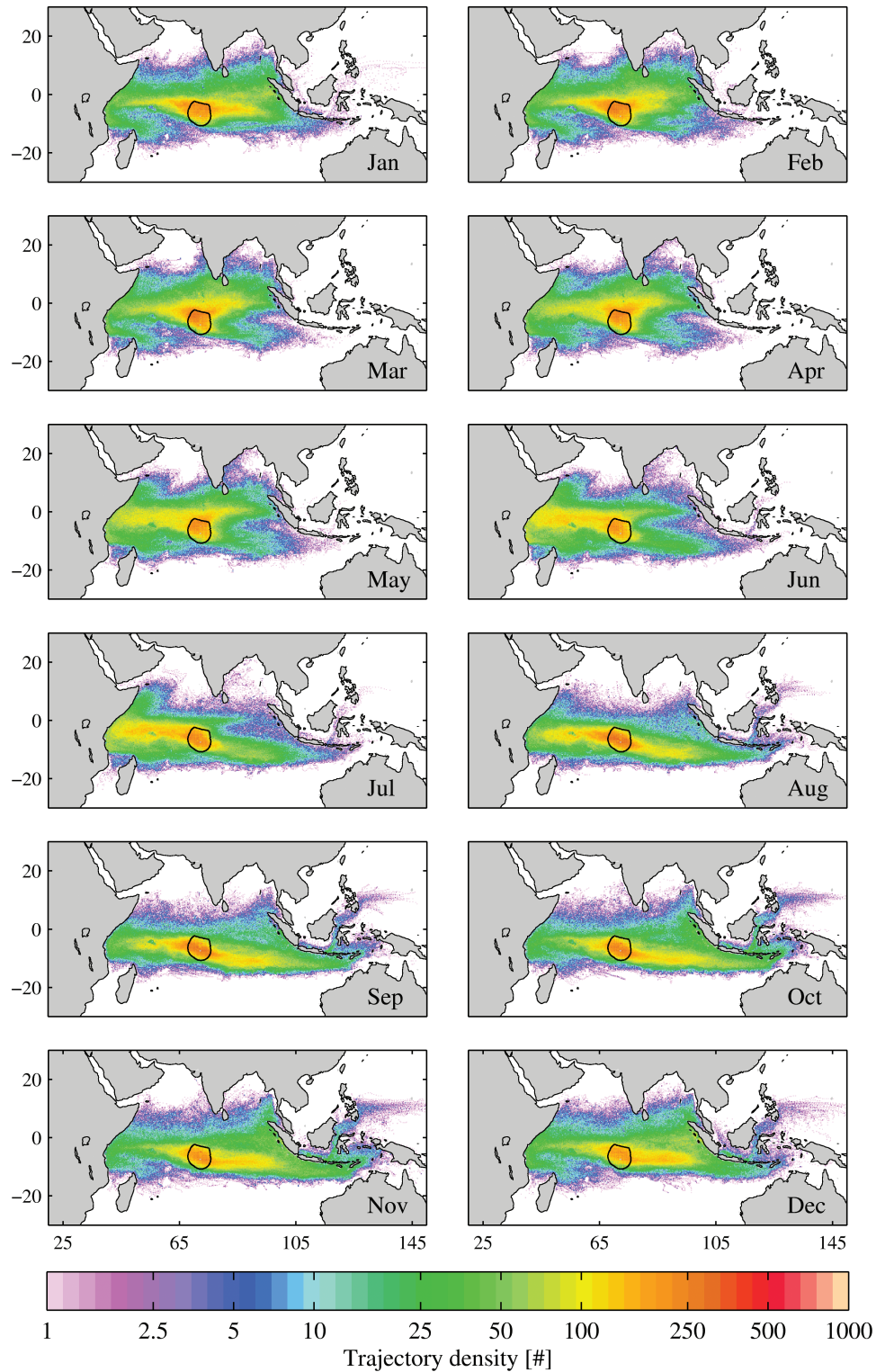


Figure 5. Census of particle advection toward the British Indian Ocean Territory marine protected area for each climatological month. Each plot includes the particles released in a given month for every year of the 10-year experiment, with an advection time of 1 year. Colors denote the cumulative “density” of particle trajectories based on their 5-daily position throughout the 10-year experiment, representing the total number of trajectories that have passed through each grid cell.

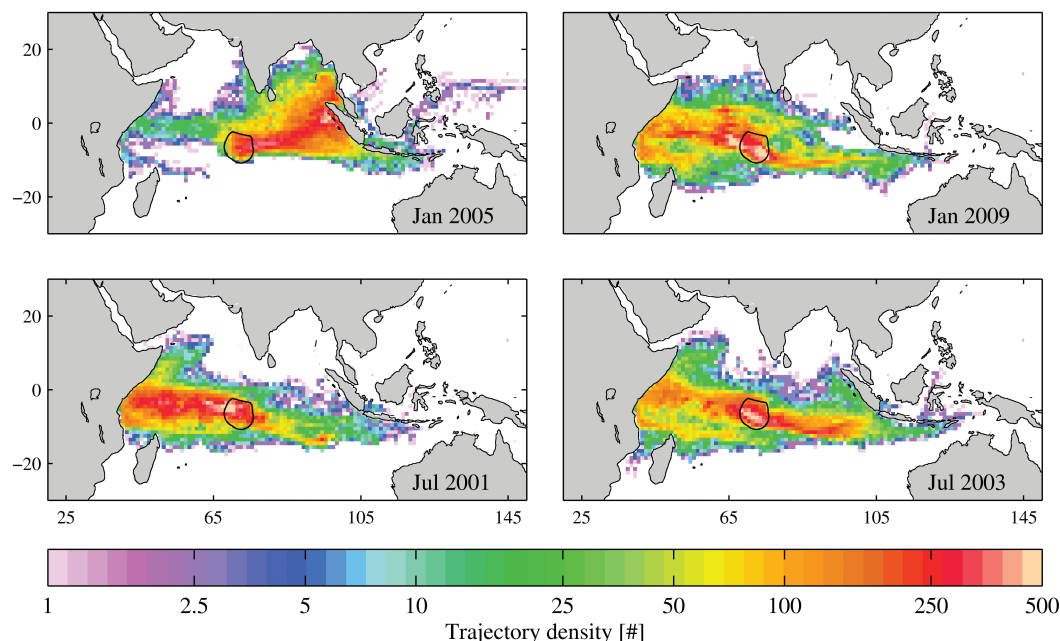


Figure 6. Census of particle advection toward the British Indian Ocean Territory marine protected area for 4 months of the experiment. The plots include the particles released in a given month for every year of the 10-year experiment, with an advection time of 1 year. Bottom left annotation details which month and year each plot represents. Colors denote the cumulative “density” of particle trajectories based on their 5-daily position throughout the 10-year experiment, representing the total number of trajectories that have passed through each grid cell.

arriving at BIOT in July for two different years. In 2001, the water is predominantly from the west, whereas in 2003 there are clear pathways from both the western and eastern sides of the Indian Ocean.

These variations in the circulation can arise as direct impacts of remote external factors, as well as from the inter-annual and seasonal variability that exists in the monsoonal wind forcing. The two principal large-scale climatological features which can impact the Indian Ocean circulation, although there are several other seasonal oscillations, are the local Indian Ocean Dipole (IOD) [Saji *et al.*, 1999], and the globally impacting ENSO [Bjerknes, 1969; Diaz *et al.*, 2001]. It is outside the scope of this work to describe these features in detail, but briefly the IOD is a shift in sea surface temperatures between the western and eastern Indian Ocean sectors, with each alternately becoming warmer and then colder in an irregular oscillation, typically lasting the boreal summer and autumn [Saji *et al.*, 1999]. The ENSO is an irregularly periodical occurrence of a warm phase (El Niño), and cool phase (La Niña) in sea surface temperatures, caused by a variation in winds over the tropical eastern Pacific Ocean, affecting much of the tropics and subtropics [Schott *et al.*, 2009]. El Niño typically lasts for 9–12 months, whereas La Niña can last for 1–3 years. There is much research and evidence of the influence of these phenomena directly on the currents of the Indian Ocean [Gnanaseelan *et al.*, 2012], indirectly via impacts on the monsoon cycle [Pillai and Chowdary, 2016], and importantly on how they interact [Luo *et al.*, 2010]. For a thorough discussion on Indian Ocean circulation variability and associated climate variability, see Schott *et al.* [2009] and references therein.

4. Discussion

4.1. Coastal Connectivity and Exposure to Human Activity

In Figure 2, it is apparent that three of the four MPAs in this study are strongly connected with land, over a 1-year timescale. Connectivity with land could be detrimental to the MPAs pristine condition, as land is the main source of pollution to the ocean, of which plastic makes up the most significant part [Shahidul Islam and Tanaka, 2004; Gall and Thompson, 2015]. Jambeck *et al.* [2015] estimated that in 2010, 275 million metric tons of plastic waste was generated in 192 coastal countries, of which 4.8–12.7 million metric tons entered the ocean (approximately 1.8–4.6%). Plastics are produced as many different varieties of polymers, and from macro to micro in size, but the key characteristic which makes plastic so commercially popular

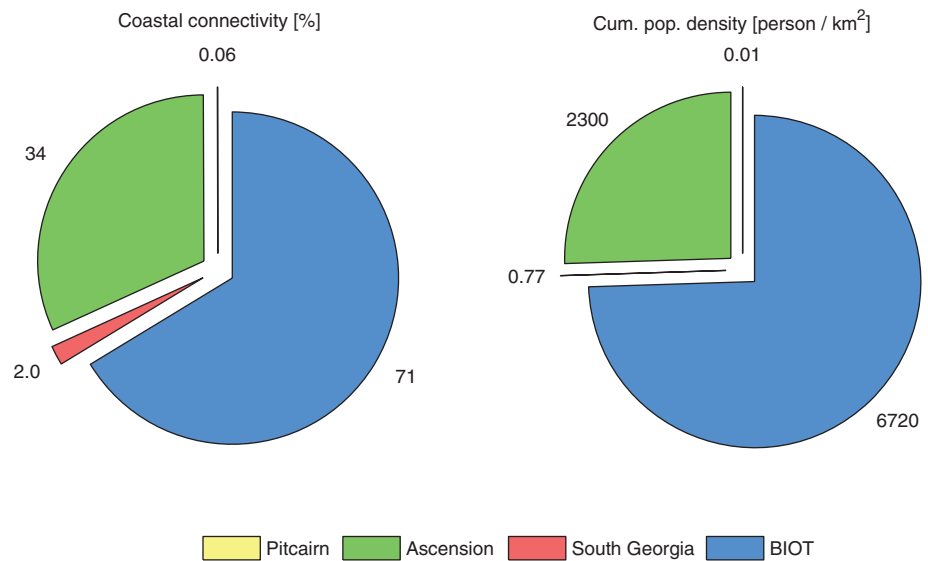


Figure 7. A comparison of the coastal connectivity and average cumulative population density encountered of water reaching each marine protected areas (MPA) over a 1 year advection period. In both cases, the charts are the averages across all 10 years of releases. The left pie chart shows the percentage of trajectories reaching each MPA that originate in coastal waters (i.e., have been within 85 km of the coast within 1 year of reaching the MPA). The right pie chart shows the corresponding average population density encountered over the same period. Both the connectivity and population density encountered of the Pitcairn MPA are too small to be clearly seen but are those at the 12 o'clock position on both charts.

is also the reason why they are so harmful and wide spread in the ocean: their durability [Cole *et al.*, 2011; United Nations Environment Programme, 2016]. Depending on the type of plastic, once in the ocean it can either sink to the ocean floor or be transported worldwide by surface currents [van Sebille *et al.*, 2015]. Most famously, there is a relatively high concentration of floating plastic, which has accumulated in so called “garbage patches” in the five sub-tropical gyres in the Indian Ocean, North and South Atlantic, and North and South Pacific [Maximenko *et al.*, 2012; Eriksen *et al.*, 2013]. Marine plastics can have significant detrimental ecological impacts, and consequently there has been much research on the impacts of both macro- and micro-plastics on biota. Direct impacts on marine species includes entanglement in macro-plastics, and ingestion of micro-plastic and subsequent absorption of toxic chemicals, namely polychlorinated biphenyls. Indirect negative impacts can come from the trophic transfer of plastics or toxins, and also floating plastic debris transporting “invader” species [Wright *et al.*, 2013; Gall and Thompson, 2015]. For a thorough synthesis on the issue of marine plastics, see [UNEP, 2016].

Having outlined the issues surrounding marine plastics, and noting the findings of [Jambeck *et al.*, 2015], who states that population size is a significant factor in the amount of plastic litter from coastal regions, we now discuss the MPAs in this context. Using the trajectory data presented in Figure 2, the percentage of trajectories that are within 85 km of the coast (the global average width of the shelf) within 1 year of release was calculated for each monthly experiment from each MPA, and presented in Tables S1–S4. The tables demonstrate the degree of seasonal and inter-annual variability discussed in Section 3, but also quantifies what is apparent in Figure 2. Over a 1 year timescale, the Pitcairn MPA is weakly connected with land, whereas of the water that flows into the South Georgia MPA, a fraction of 2% originates from the coast, a fraction of 34% for Ascension, and 71% for BIOT (see Figure 7).

However, connectivity with land is only significant for the MPAs if the land is highly populated and, thus, vulnerable in terms of pollution [Jambeck *et al.*, 2015]. In Figure 2, the land is filled with population density data [CIESIN, FAO, CIAT, 2005], and we now use this to further assess the impact-potential of trajectories originating from the coast. As is apparent in Figure 2, India, and parts of Indonesia and Africa, have the highest population densities of the regions that are connected with the MPAs, most notably to BIOT in the Indian Ocean. To quantify this, Tables S5–S8 in the supplementary material detail the average cumulative population density (persons/km²) encountered by the circulation pathways, from each monthly experiment for each year for each MPA (Figure S8 shows time series of population density encountered as average across

all trajectories and the corresponding cumulative average). This information is important, since, even if only a small fraction of the pathways that reach a MPA have been in close proximity to land, they can be significant if the coast is relatively densely populated. While Tables S5–S8 report cumulative numbers averaged across all trajectories, the highest population density encountered by South Georgia pathways, was 3,134 person/km², originating from the coastal cities of the State of São Paulo; for Ascension, 5,288 person/km², originating from the coastal region of Lagos; and for the BIOT MPA, 15,203 person/km², originating from the coastal region of Mumbai. By contrast, trajectories reaching Pitcairn had encountered only a maximum of 34 person/km² in the preceding year.

We note that this approach is a simplification, assuming that a high population density equates to high levels of pollution. In reality, the situation is more complex and depends on the economic status of the coastal region which can determine factors such as the quality of waste management systems [Jambeck *et al.*, 2015]. Nevertheless, we use this approach as a first-order approximation of the possible pollution risk as a consequence of coastal connectivity. We also note that a large proportion of plastics which enter the marine environment do not float, and therefore would not impact the MPAs via circulation connectivity.

4.1.1. Four of a Kind?

Having outlined the average coastal connectivity, and the population density encountered by the MPA pathways, Figure 7 presents this information for cross-comparison of each MPA over a 1 year advection period.

Focusing first on the Pitcairn MPA in Figure 7, it is immediately apparent that the model suggests there is no risk of coastal pollution via ocean circulation. The South Georgia MPA has a very low coastal connectivity fraction (2%), however, the coasts that it is connected with include the relatively highly populated southeast coast of Brazil. Nevertheless, with such a low coastal connectivity the exposure to coastal pollution is low. The Ascension MPA, has an coastal connectivity of 34%, of which the average cumulative population density encountered over 1 year is 2,300 person/km². As such, the Ascension MPA is exposed to a significant pollution risk via ocean circulation. This is a particular threat to the islands important rookery for the endangered green turtle [Petit and Prudent, 2010], as the juveniles can perish by ingesting less than 1 g of marine debris [Santos *et al.*, 2015]. Finally, the BIOT MPA is the most vulnerable to coastal pollution via ocean circulation of all the MPAs in this study, as it has both the highest coastal connectivity, at 71%, and population density encountered, at 6,720 person/km². The BIOT MPA is comprised of 55 coral islands spread between five atolls, with more than 220 species of coral, and is currently considered to be one of the best preserved reefs in the world [Sheppard *et al.*, 2012]. However, the high degree of exposure to densely populated coastlines shown here, together with the discovery that corals are ingesting micro-plastics [Hall *et al.*, 2015], suggest that the pristine condition of the BIOT corals may be under threat.

4.2. Further Negative Impacts of Connectivity

This paper has focused on the pollution threat from land, specifically discussing plastic, however, connectivity with the coast and marine plastics are not the only issue. Many other human activities take place in the ocean, from which a variety of hazards to the marine environment can arise. Here, we will briefly discuss other threats to MPAs through their connectivity, namely issues associated with shipping, oil spills, and fishing.

The industrial-scale shipping of cargo, which makes up 90% of world trade movement [Kaluza *et al.*, 2010], takes the risks associated with human activity out into the open ocean, across all major ocean basins. Although the MARPOL 73/78 Convention [Lethbridge, 1991] was developed to prevent or minimize operational or accidental discharges of pollutants from vessels at sea (though restrictions largely stop 12 nautical miles offshore), these remain significant. For instance, an early estimate from 1982 reported that as many as 600,000 plastic containers worldwide were being dumped at sea per day from shipping [Wace, 1995], and there remains significant daily disposal of onboard garbage and sewage from both commercial and tourism ships [Shahidul Islam and Tanaka, 2004]. In addition to marine litter, there is the threat of oil spills, which are rare but devastating. One of the most public and notorious spills, was the Exxon Valdez oil tanker spill in 1989, which emitted 41.6 million liters of oil, and had a dramatic impact on Alaskan wildlife [Atlas and Hazen, 2011]. The incident killed more than 30,000 birds of 90 different species in just over 4 months [Piatt *et al.*, 1990]. Over 25 years on since the disaster, and the effect on the marine environment is still being felt, through the persistence of toxic sub-surface oil and chronic exposure resulting in delayed

population reductions and cascades of indirect effects [Peterson *et al.*, 2003]. A final known threat strongly associated with shipping, is marine bioinvasion. The two major routes by which invasive species spread, is via discharged water from ships' ballast tanks [Ruiz *et al.*, 2000] and hull fouling [Drake and Lodge, 2007]. In several parts of the world, invasive species have caused species extinction and habitat alteration [Mack *et al.*, 2000]. Kaluza *et al.* [2010] produced a network map of global ship movements (their Figure 1), the style of which can be overlaid with an MPAs connectivity footprint, to show which major shipping routes could potentially affect the MPAs, either through an oil spill disaster or increasing exposure to marine litter or invasive species.

The threat of oil spills is not solely limited to shipping incidents, there can also be rare but catastrophic spills from oil wells, the most famous recently being the Deepwater Horizon Oil Spill in 2010. The oil from the spill, 779 million liters [Atlas and Hazen, 2011], was spread across the Gulf of Mexico region by ocean circulation [Liu *et al.*, 2011], with 847 km of shoreline still contaminated 1 year after the spill despite clean up efforts [Michel *et al.*, 2013]. In the aftermath of this disaster, similar methods to that used here have been used to calculate the "circulation footprint" from possible oil spills, in order to reduce risk through better response and improved situational awareness [Main *et al.*, 2017]. This approach, in combination with the results presented here, can enable MPA managers to likewise be more aware of potential oil spill risks within their connectivity footprint, and consequently be prepared in the event of a spill.

Fishing activities provide both direct pressure on marine ecosystems as well as indirect pressures from marine littering, such as fishing tackle [Shahidul Islam and Tanaka, 2004]. Marine species can have various stages to their life cycles, which can involve larval dispersal during a pelagic stage. Dispersal via ocean currents determines the connectivity of local populations and therefore the knowledge and understanding of it is vital for conservation strategies [Mora and Sale, 2002]. Unless a system is efficiently self-sustaining (retainment exceeds or equals overspill), overfishing in one region, can impact populations downstream, and consequently even remote MPA ecosystems could be vulnerable. [Figueira, 2009] looked at identifying "patches" as either sources or sinks within a metapopulation, in order to more effectively designate marine reserves. Knowing a location's contribution to the ecosystem, and using the MPA connectivity footprints, can help fill in the knowledge gaps of population connectivity, and aid in the spatial management of protection efforts at time scales relevant to the pelagic larval duration of the species of interest [Sale *et al.*, 2005].

4.3. Future Work

In this study, we have produced a 1 year connectivity "footprint" for each MPA, and used it to assess connectivity with land. However, as discussed in the Section 4.2, pollution is not restricted to the coast, there are various other sources of potential hazards. The connectivity footprints produced in this study could be compared with other risk factors, such as shipping lanes, oil rigs, or fishing grounds, similar to the global human impact study by Halpern *et al.* [2008]. Additionally, the work here focuses on a timescale of 1 year, but a more detailed study of the timescales of particular risks could be considered. This would fully assess the pollution threat, and or, ecological implications posed to each MPA through connectivity.

In the introduction, the implications of downstream (forward) connectivity were introduced, namely seeding species to other areas. In order to seed species downstream, the timescale of connectivity is crucial, as the pelagic larval duration of the species needs to be equal to or greater than the connectivity timescale [Cowen *et al.*, 2007; Gawarkiewicz *et al.*, 2007]. The methodology and analysis used in this study can be performed in exactly the same way, but with forward Lagrangian particle tracking, enabling the timescales of downstream connectivity to be determined. Forward connectivity footprints, in addition to the backward connectivity footprints, would be extremely useful in the formation of networks, or ecological zones of MPAs, to protect ecological processes and areas that are necessary for the full life cycle of marine species [Halpern, 2003]; The World Bank, 2006]. Additionally, this could also be a tool to aid marine spatial planning, as there are increasing calls for the integration of MPAs with fisheries management to aid global biodiversity [Gell and Roberts, 2003; Hilborn, 2016].

One final consideration, whether considering the forward or backward circulation connectivity of MPAs, is the potential for the circulation itself to change, under the stress of climate change. Observations show that the intensity and position of western boundary currents are already changing [Wu *et al.*, 2012; Yang *et al.*, 2016]. Also, a model projection has forecast further deviations in the circulation between the 2000–2010

and 2050–2059 decadal averages [Popova *et al.*, 2016]. In order to assess the impact such circulation changes may impose on ocean ecosystems, such as on the connectivity, nutrient pathways, and migration of species, further in-depth Lagrangian study using model future projections would be required.

5. Summary

- MPAs are typically established to conserve important ecosystems and protect marine species, but their success in achieving these goals requires evaluation, particularly with regard to their vulnerability to upstream impacts.
- Here, we present the “connectivity footprints” of four MPAs, for a timescale of 1 year, using a Lagrangian particle-tracking technique within a high-resolution ocean GCM, and specifically consider their connectivity with land.
- Over a 1 year timescale, Pitcairn MPA is essentially unconnected with land, whereas of the water that flows into the South Georgia MPA, around 2% originates from the coast, with 34% for Ascension, and 71% for BIOT, with variability (both seasonal and inter-annual) found to be notably high for BIOT.
- Population density of the connected coastlines is considered in terms of exposure to pollution, specifically plastics, and identified as a coastal connectivity risk that needs to be considered in the management of MPAs.
- Further risks to MPAs, associated with open-ocean connectivity, namely shipping, oil spills, and fishing, are discussed and highlight the potential use of the connectivity footprint in relation to these threats.
- We advocate connectivity footprints of MPAs should be used as a tool to improve future MPA designation, and in spatial planning of current MPA networks, and suggest future work to improve the diagnosis of connectivity footprints of MPAs.

References

Acknowledgments

This study was carried out using the computational tool Ariane, developed by B. Blanke and N. Grima, available at <http://stockage.univ-brest.fr/grima/Ariane/ariane.html>. The 1/12° NEMO simulation used in this work was produced using the ARCHER UK National Supercomputing Service (<http://www.archer.ac.uk>), and is available at <http://gws-access.ceda.ac.uk/public/nemo/>. This work was funded by the UK Natural Environment Research Council through a PhD studentship for J.R. (NE/K500938/1), and national capability funding for A.L.N., E.E.P., M.A.S., and A.Y. The model output generated during this study is available upon request to the communicating author A.Y. (axy@noc.ac.uk).

- Alexander, D., and G. Osborne (2015), *Budget 2015*, pp. 124, HM Treasury, London, U. K.
- Atlas, R. M., and T. C. Hazen (2011), Oil biodegradation and bioremediation: A tale of the two worst spills in U.S. history, *Environ. Sci. Technol.*, 45(16), 6709–6715. <https://doi.org/10.1021/es2013227>.
- Avagliano, E., A. Bocquet, and J. Kape (2015), *Pitcairn Islands Ecosystem Profile*, pp. 53, Comité français de l'UICN, Paris, France.
- Barner, A., J. Lubchenco, C. Costello, S. Gaines, A. Leland, B. Jenks, S. Murawski, E. Schwaab, and M. Spring (2015), Solutions for recovering and sustaining the bounty of the ocean: Combining fishery reforms, rights-based fisheries management, and marine reserves, *Oceanography*, 25(2), 252–263. <https://doi.org/10.5670/oceanog.2015.51>.
- Bjerknes, J. (1969), Atmospheric teleconnections from the equatorial Pacific, *Mon. Weather Rev.*, 97, 163–172. [https://doi.org/10.1175/1520-0493\(1969\)097<0163:atftpe>2.3.co;2](https://doi.org/10.1175/1520-0493(1969)097<0163:atftpe>2.3.co;2).
- Blanke, B., and S. Raynaud (1997), Kinematics of the Pacific equatorial undercurrent: An Eulerian and Lagrangian approach from GCM results, *J. Phys. Oceanogr.*, 27(6), 1038–1053. [https://doi.org/10.1175/1520-0485\(1997\)027<1038:KOTPEU>2.0.CO;2](https://doi.org/10.1175/1520-0485(1997)027<1038:KOTPEU>2.0.CO;2).
- Blanke, B., M. Arhan, G. Madec, and S. Roche (1999), Warm water paths in the equatorial Atlantic as diagnosed with a general circulation model, *J. Phys. Oceanogr.*, 29(11), 2753–2768. [https://doi.org/10.1175/1520-0485\(1999\)029<2753:wwppte>2.0.co;2](https://doi.org/10.1175/1520-0485(1999)029<2753:wwppte>2.0.co;2).
- BLUE Marine Foundation (2016), *2016 Begins With the Creation of the Largest Marine Reserve in Atlantic Ocean*, edited by C. Clover, BLUE Mar. Found., London, U. K.
- Brandt, P., A. Funk, A. Tantet, W. E. Johns, and J. Fischer (2014), The equatorial undercurrent in the central Atlantic and its relation to tropical Atlantic variability, *Clim. Dyn.*, 43(11), 2985–2997. <https://doi.org/10.1007/s00382-014-2061-4>.
- Brodeau, L., B. Barnier, A.-M. Treguier, T. Penduff, and S. Gulev (2010), An ERA40-based atmospheric forcing for global ocean circulation models, *Ocean Model.*, 31(3–4), 88–104. <https://doi.org/10.1016/j.ocemod.2009.10.005>.
- Center for International Earth Science Information Network, Columbia University United Nations, Food Agriculture Programme Centro Internacional de Agricultura Tropical (2005), *Gridded Population of the World, Version 3 (GPWv3): Population Count Grid, Future Estimates*, NASA Socioecon. Data and Appl. Center (SEDAC), Palisades, N. Y. <https://doi.org/10.7927/h42B8vzz>.
- Christie, P. and A. T. White (2007), Best practices in governance and enforcement of marine protected areas: An overview, *Rep. for the Workshop on Marine Protected Areas and Fisheries Management: Review of Issues and Considerations*, pp. 183–220, Rome, Italy.
- Christie, M. R., B. N. Tissot, M. A. Albins, J. P. Beets, Y. Jia, D. M. Ortiz, S. E. Thompson, and M. A. Hixon (2010), Larval connectivity in an effective network of marine protected areas, *PLoS One*, 5(12), e15715. <https://doi.org/10.1371/journal.pone.0015715>.
- Cole, M., P. Lindeque, C. Halsband, and T. S. Galloway (2011), Microplastics as contaminants in the marine environment: A review, *Mar. Pollut. Bull.*, 62(12), 2588–2597. <https://doi.org/10.1016/j.marpolbul.2011.09.025>.
- Collins, M. (2013), *Press Release: New Spatial and Temporal Closed Areas Added to the South Georgia and the South Sandwich Islands Marine Protected Area*, Government of South Georgia and the South Sandwich Islands, Govern. House, Stanley, Falkland Islands.
- Constable, A. J., et al. (2014), Climate change and Southern Ocean ecosystems I: How changes in physical habitats directly affect marine biota, *Glob. Change Biol.*, 20(10), 3004–3025. <https://doi.org/10.1111/gcb.12623>.
- Cowen, R. K., G. Gawarkiewicz, J. Pineda, S. R. Thorrold, and F. E. Werner (2007), Population connectivity in marine systems: An overview, *Oceanography*, 20(3), 14–21. <https://doi.org/10.5670/oceanog.2007.26>.
- Day, J., N. Dudley, M. Hockings, G. Holmes, D. Laffoley, S. Stolton, and S. Wells (2012), *Guidelines for Applying the IUCN Protected Area Management Categories to Marine Protected Areas*, IUCN, Gland, Switzerland.
- Diaz, H. F., M. P. Hoerling, and J. K. Eischeid (2001), ENSO variability, teleconnections and climate change, *Int. J. Climatol.*, 21(15), 1845–1862. <https://doi.org/10.1002/joc.631>.
- Doney, S., L. Bopp, and M. Long (2014), Historical and future trends in ocean climate and biogeochemistry, *Oceanography*, 27(1), 108–119. <https://doi.org/10.5670/oceanog.2014.14>.

- Drake, J. M., and D. M. Lodge (2007), Hull fouling is a risk factor for intercontinental species exchange in aquatic ecosystems, *Aquat. Invasions*, 2(2), 121–131. <https://doi.org/10.3391/ai.2007.2.2.7>.
- Dudley, N. (Ed) (2008), *Guidelines for Applying Protected Area Management Categories*, IUCN, Gland, Switzerland.
- Edgar, G. J., et al. (2014), Global conservation outcomes depend on marine protected areas with five key features, *Nature*, 506(7487), 216–220. <https://doi.org/10.1038/nature13022>.
- Elrod, V. A., W. M. Berelson, K. H. Coale, and K. S. Johnson (2004), The flux of iron from continental shelf sediments: A missing source for global budgets, *Geophys. Res. Lett.*, 31(12), L12307. <https://doi.org/10.1029/2004gl020216>.
- Eriksen, M., N. Maximenko, M. Thiel, A. Cummins, G. Lattin, S. Wilson, J. Hafner, A. Zellers, and S. Rifman (2013), Plastic pollution in the South Pacific subtropical gyre, *Mar. Pollut. Bull.*, 68(1–2), 71–76. <https://doi.org/10.1016/j.marpolbul.2012.12.021>.
- Fiedler, P. C., and L. D. Talley (2006), Hydrography of the eastern tropical Pacific: A review, *Prog. Oceanogr.*, 69(2–4), 143–180. <https://doi.org/10.1016/j.pocean.2006.03.008>.
- Figueira, W. F. (2009), Connectivity or demography: Defining sources and sinks in coral reef fish metapopulations, *Ecol. Model.*, 220(8), 1126–1137. <https://doi.org/10.1016/j.ecolmodel.2009.01.021>.
- Fogarty, M. J., and L. W. Botsford (2007), Population connectivity and spatial management of marine fisheries, *Oceanography*, 20(3), 112–123. <https://doi.org/10.5670/oceanog.2007.34>.
- Friedlander, A. M., J. E. Caselle, E. Ballesteros, E. K. Brown, A. Turchik, and E. Sala (2014), The real bounty: Marine biodiversity in the Pitcairn Islands, *PLoS One*, 9(6), e100142. <https://doi.org/10.1371/journal.pone.0100142>.
- Gall, S. C., and R. C. Thompson (2015), The impact of debris on marine life, *Mar. Pollut. Bull.*, 92(1–2), 170–179. <https://doi.org/10.1016/j.marpolbul.2014.12.041>.
- Gawarkiewicz, G., S. Monismith, and J. Largier (2007), Observing larval transport processes affecting population connectivity progress and challenges, *Oceanography*, 20(3), 40–53. <https://doi.org/10.5670/oceanog.2007.28>.
- Gell, F. R., and C. M. Roberts (2003), Benefits beyond boundaries: The fishery effects of marine reserves, *Trends Ecol. Evol.*, 18(9), 448–455. [https://doi.org/10.1016/s0169-5347\(03\)00189-7](https://doi.org/10.1016/s0169-5347(03)00189-7).
- Gnanaseelan, C., A. Deshpande, and M. J. McPhaden (2012), Impact of Indian Ocean Dipole and El Niño/southern oscillation wind-forcing on the Wyrtki jets, *J. Geophys. Res. Oceans*, 117(C8), C08005. <https://doi.org/10.1029/2012jc007918>.
- Goes, M., R. Molinari, I. da Silveira, and I. Wainer (2005), Retroreflections of the North Brazil Current during February 2002, *Deep-Sea Res. I Oceanogr. Res. Pap.*, 52(4), 647–667. <https://doi.org/10.1016/j.dsr.2004.10.010>.
- Golden, C. D., E. H. Allison, W. W. L. Cheung, M. M. Dey, B. S. Halpern, D. J. McCauley, M. Smith, B. Vaitla, D. Zeller, and S. S. Myers (2016), Fall in fish catch threatens human health, *Nature*, 534, 317–320. <https://doi.org/10.1038/534317a>.
- Grenier, M., S. Cravatte, B. Blanke, C. Menkes, A. Koch-Larrouy, F. Durand, A. Melet, and C. Jeandel (2011), From the western boundary currents to the Pacific equatorial undercurrent: Modeled pathways and water mass evolutions, *J. Geophys. Res.*, 116(C12), 1–16. <https://doi.org/10.1029/2011jc007477>.
- Guitart, C., A. Sheppard, T. Frickers, A. R. Price, and J. W. Readman (2007), Negligible risks to corals from antifouling booster biocides and triazine herbicides in coastal waters of the Chagos Archipelago, *Mar. Pollut. Bull.*, 54(2), 226–232. <https://doi.org/10.1016/j.marpolbul.2006.10.012>.
- Hall, N. M., K. L. E. Berry, L. Rintoul, and M. O. Hoogenboom (2015), Microplastic ingestion by scleractinian corals, *Mar. Biol.*, 162(3), 725–732. <https://doi.org/10.1007/s00227-015-2619-7>.
- Halpern, B. S. (2003), The impact of marine reserves: Do reserves work and does reserve size matter? *Ecol. Appl.*, 13(1), S117–S137. [https://doi.org/10.1890/1051-0761\(2003\)013\[0117:tiomrd\]2.0.co;2](https://doi.org/10.1890/1051-0761(2003)013[0117:tiomrd]2.0.co;2).
- Halpern, B. S., et al. (2008), A global map of human impact on marine ecosystems, *Science*, 319(5865), 948–952. <https://doi.org/10.1126/science.1149345>.
- Hilborn, R. (2016), Marine biodiversity needs more than protection, *Nature*, 535, 224–226. <https://doi.org/10.1038/535224a>.
- International Union for Conservation of Nature (IUCN), and United Nations Environment Programme-World Conservation Monitoring Centre (UNEP-WCMC) (2013), *The World Database on Protected Areas (WDPA)*, UNEP-WCMC, Cambridge, U. K. [Available at: <https://www.protectedplanet.net/>].
- Jambeck, J. R., R. Geyer, C. Wilcox, T. R. Siegler, M. Perryman, A. Andrady, R. Narayan, and K. L. Law (2015), Marine pollution. Plastic waste inputs from land into the ocean, *Science*, 347(6223), 768–771. <https://doi.org/10.1126/science.1260352>.
- Jameson, S. C., M. H. Tupper, and J. M. Ridley (2002), The three screen doors: Can marine “protected” areas be effective? *Mar. Pollut. Bull.*, 44(11), 1177–1183. [https://doi.org/10.1016/s0025-326x\(02\)00258-8](https://doi.org/10.1016/s0025-326x(02)00258-8).
- Johnson, E. S., F. Bonjean, G. S. E. Lagerloef, J. T. Gunn, and G. T. Mitchum (2007), Validation and error analysis of OSCAR sea surface currents, *J. Atmos. Oceanic Tech.*, 24(4), 688–701. <https://doi.org/10.1175/jtech1971.1>.
- Jonsson, B. F., and J. R. Watson (2016), The timescales of global surface-ocean connectivity, *Nat. Commun.*, 7, 11239. <https://doi.org/10.1038/ncomms11239>.
- Kaluza, P., A. Kolzsch, M. T. Gastner, and B. Blasius (2010), The complex network of global cargo ship movements, *J. R. Soc. Interface*, 7(48), 1093–1103. <https://doi.org/10.1098/rsif.2009.0495>.
- Lass, H. U., M. Schmidt, V. Mohrholz, and G. Nausch (2000), Hydrographic and current measurements in the area of the Angola–Benguela Front, *J. Phys. Oceanogr.*, 30, 2589–2609. [https://doi.org/10.1175/1520-0485\(2000\)030<2589:hacmit>2.0.co;2](https://doi.org/10.1175/1520-0485(2000)030<2589:hacmit>2.0.co;2).
- Lethbridge, J. R. (1991), MARPOL 73/78 (International Convention for the Prevention of Pollution from Ships), *Infrastructure Notes, No. PS-4*, World Bank, Washington, D. C.
- Liu, Y., R. H. Weisberg, C. Hu, and L. Zheng (2011), Tracking the deepwater horizon oil spill: A modeling perspective, *Eos. Trans. AGU*, 92(6), 45–52. <https://doi.org/10.1029/2011EO060001>.
- Locarnini, R. A., et al. (2013), in *World Ocean Atlas 2013, Volume 1: Temperature*, edited by S. Levitus and A. Mishonov (technical editor), NOAA Atlas NESDIS 73.
- Lunn, J. (2016), Disputes over the British Indian Ocean Territory: April 2016 update, *Commons Briefing Papers SN06908*, edited by House of Commons.
- Luo, J.-J., R. Zhang, S. K. Behera, Y. Masumoto, F.-F. Jin, R. Lukas, and T. Yamagata (2010), Interaction between El Niño and extreme Indian ocean dipole, *J. Clim.*, 23(3), 726–742. <https://doi.org/10.1175/2009jcli3104.1>.
- Mack, R. N., D. Simberloff, W. M. Lonsdale, H. Evans, M. Clout, and F. A. Bazzaz (2000), Biotic invasions: Causes, epidemiology, global consequences, and control, *Ecol. Appl.*, 10, 689–710. [https://doi.org/10.1890/1051-0761\(2000\)010](https://doi.org/10.1890/1051-0761(2000)010).
- Maes, C., B. Blanke, and E. Martinez (2016), Origin and fate of surface drift in the oceanic convergence zones of the eastern Pacific, *Geophys. Res. Lett.*, 43, 3398–3405. <https://doi.org/10.1002/2016GL068217>.

- Main, C. E., A. Yool, N. P. Holliday, E. E. Popova, D. O. B. Jones, and H. A. Ruhl (2017), Simulating pathways of subsurface oil in the Faroe–Shetland Channel using an ocean general circulation model, *Mar. Pollut. Bull.*, *114*, 315–326. <https://doi.org/10.1016/j.marpolbul.2016.09.041>.
- Marzocchi, A., J. J.-M. Hirschi, N. P. Holliday, S. A. Cunningham, A. T. Blaker, and A. C. Coward (2014), The North Atlantic subpolar circulation in an eddy-resolving global ocean model, *J. Mar. Syst.*, *142*, 126–143. <https://doi.org/10.1016/j.jmarsys.2014.10.007>.
- Maximenko, N., J. Hafner, and P. Niiler (2012), Pathways of marine debris derived from trajectories of Lagrangian drifters, *Mar. Pollut. Bull.*, *65*(1–3), 51–62. <https://doi.org/10.1016/j.marpolbul.2011.04.016>.
- Meyers, G., R. J. Bailey, and A. P. Worby (1995), Geostrophic transport of Indonesian throughflow, *Deep-Sea Res. I*, *42*(7), 1163–1174. [https://doi.org/10.1016/0967-0637\(95\)00037-7](https://doi.org/10.1016/0967-0637(95)00037-7).
- Michel, J., et al. (2013), Extent and degree of shoreline oiling: Deepwater horizon oil spill, Gulf of Mexico, USA, *PLoS One*, *8*(6), e65087. <https://doi.org/10.1371/journal.pone.0065087>.
- Mills, K., et al. (2013), Fisheries management in a changing climate: Lessons from the 2012 ocean heat wave in the Northwest Atlantic, *Oceanography*, *26*(2), 191–195. <https://doi.org/10.5670/oceanog.2013.27>.
- Mora, C., and P. F. Sale (2002), Are populations of coral reef fish open or closed? *Trends Ecol. Evol.*, *17*(9), 422–428. [https://doi.org/10.1016/S0169-5347\(02\)02584-3](https://doi.org/10.1016/S0169-5347(02)02584-3).
- Murphy, E. J., et al. (2013), Comparison of the structure and function of Southern Ocean regional ecosystems: The Antarctic Peninsula and South Georgia, *J. Mar. Syst.*, *109–110*, 22–42. <https://doi.org/10.1016/j.jmarsys.2012.03.011>.
- Myers, N., R. A. Mittermeier, C. G. Mittermeier, G. A. da Fonseca, and J. Kent (2000), Biodiversity hotspots for conservation priorities, *Nature*, *403*(6772), 853–858. <https://doi.org/10.1038/35002501>.
- Nash, J., E. Shroyer, S. Kelly, M. Inall, T. Duda, M. Levine, N. Jones, and R. Musgrave (2012), Are any coastal internal tides predictable? *Oceanography*, *25*(2), 80–95. <https://doi.org/10.5670/oceanog.2012.44>.
- New, A. L., S. G. Alderson, D. A. Smeed, and K. L. Stansfield (2007), On the circulation of water masses across the Mascarene Plateau in the South Indian Ocean, *Deep-Sea Res. I*, *54*, 42–74. <https://doi.org/10.1016/j.dsr.2006.08.016>.
- Partelow, S., H. von Wehrden, and O. Horn (2015), Pollution exposure on marine protected areas: A global assessment, *Mar. Pollut. Bull.*, *100*(1), 352–358. <https://doi.org/10.1016/j.marpolbul.2015.08.026>.
- Pauly, D., R. Watson, and J. Alder (2005), Global trends in world fisheries: Impacts on marine ecosystems and food security, *Philos. Trans. R. Soc. Lond. B Biol. Sci.*, *360*(1453), 5–12. <https://doi.org/10.1098/rstb.2004.1574>.
- Pelembé, T., and G. Cooper (Eds) (2011), *UK Overseas Territories and Crown Dependencies: 2011 Biodiversity Snapshot*, Joint Nat. Conserv. Comm., Peterborough, U. K.
- Peterson, R. G., and L. Stramma (1991), Upper-level circulation in the South Atlantic Ocean, *Progr. Oceanogr.*, *26*, 1–73. [https://doi.org/10.1016/0079-6611\(91\)90006-8](https://doi.org/10.1016/0079-6611(91)90006-8).
- Peterson, C. H., S. D. Rice, J. W. Short, D. Esler, J. L. Bodkin, B. E. Ballachey, and D. B. Irons (2003), Long-term ecosystem response to the Exxon Valdez oil spill, *Science*, *302*(5653), 2082–2086. <https://doi.org/10.1126/science.1084282>.
- Petit, J., and G. Prudent (2010), *Climate Change and Biodiversity in the European Union Overseas Entities*, 192 pp., IUCN, Gland, Switzerland and Brussels, Belgium.
- Piatt, J. F., C. J. Lensink, W. Butler, K. Marshal, and D. R. Nysewander (1990), Immediate impact of the 'Exxon Valdez' oil spill on marine birds, *Auk*, *107*(2), 387–397. <https://doi.org/10.2307/4087623>.
- Pillai, P. A., and J. S. Chowdary (2016), Indian summer monsoon intra-seasonal oscillation associated with the developing and decaying phase of El Niño, *Int. J. Climatol.*, *36*(4), 1846–1862. <https://doi.org/10.1002/joc.4464>.
- Popova, E., et al. (2016), From global to regional and back again: Common climate stressors of marine ecosystems relevant for adaptation across five ocean warming hotspots, *Glob. Change Biol.*, *22*(6), 2038–2053. <https://doi.org/10.1111/gcb.13247>.
- Richardson, P. L., S. Arnault, S. Garzoli, and J. G. Bruce (1992), Annual cycle of the Atlantic North Equatorial Countercurrent, *Deep-Sea Res.*, *39*(6), 997–1014. [https://doi.org/10.1016/0198-0149\(92\)90036-s](https://doi.org/10.1016/0198-0149(92)90036-s).
- Rintoul, S. R., C. Hughes, and D. Olbers (2001), The Antarctic circumpolar current system, in *Ocean Circulation and Climate: Observing and Modelling the Global Ocean*, edited by G. Siedler, J. Church, and J. Gould, pp. 271–302, Acad. Press, London, U. K.
- Robinson, J., E. E. Popova, A. Yool, M. Srokosz, R. S. Lampitt, and J. R. Blundell (2014), How deep is deep enough? Ocean iron fertilization and carbon sequestration in the Southern Ocean, *Geophys. Res. Lett.*, *41*(7), 2489–2495. <https://doi.org/10.1002/2013GL058799>.
- Ruiz, G. M., T. K. Rawlings, F. C. Dobbs, L. A. Drake, T. Mullady, A. Huq, and R. R. Colwell (2000), Global spread of microorganisms by ships, *Nature*, *408*, 49–50. <https://doi.org/10.1038/35040695>.
- Saji, N. H., B. N. Goswami, P. N. Vinayachandran, and T. Yamagata (1999), A dipole mode in the tropical Indian Ocean, *Nature*, *401*(6751), 360–363. <https://doi.org/10.1038/43854>.
- Sale, P. F., et al. (2005), Critical science gaps impede use of no-take fishery reserves, *Trends Ecol. Evol.*, *20*(2), 74–80. <https://doi.org/10.1016/j.tree.2004.11.007>.
- Santos, R. G., R. Andrades, M. A. Boldrini, and A. S. Martins (2015), Debris ingestion by juvenile marine turtles: An underestimated problem, *Mar. Pollut. Bull.*, *93*(1–2), 37–43. <https://doi.org/10.1016/j.marpolbul.2015.02.022>.
- Schott, F. A., and J. P. McCreary (2001), The monsoon circulation of the Indian Ocean, *Prog. Oceanogr.*, *51*(1), 1–123. [https://doi.org/10.1016/S0079-6611\(01\)00083-0](https://doi.org/10.1016/S0079-6611(01)00083-0).
- Schott, F. A., S.-P. Xie, and J. P. McCreary (2009), Indian Ocean circulation and climate variability, *Rev. Geophys.*, *47*(1), RG1002. <https://doi.org/10.1029/2007rg000245>.
- van Sebille, E., C. Wilcox, L. Lebreton, N. Maximenko, B. D. Hardesty, J. A. van Franeker, M. Eriksen, D. Siegel, F. Galgani, and K. L. Law (2015), A global inventory of small floating plastic debris, *Environ. Res. Lett.*, *10*(12), 124006. <https://doi.org/10.1088/1748-9326/10/12/124006>.
- Secretariat of the Convention on Biological Diversity (2014), *Global Biodiversity Outlook 4*, Secr. of the Conv. on Biol. Divers., Montreal, Canada.
- Shahidul Islam, M., and M. Tanaka (2004), Impacts of pollution on coastal and marine ecosystems including coastal and marine fisheries and approach for management: A review and synthesis, *Mar. Pollut. Bull.*, *48*(7–8), 624–649. <https://doi.org/10.1016/j.marpolbul.2003.12.004>.
- Shankar, D., P. N. Vinayachandran, and A. S. Unnikrishnan (2002), The monsoon currents in the north Indian Ocean, *Prog. Oceanogr.*, *52*(1), 63–120. [https://doi.org/10.1016/S0079-6611\(02\)00024-1](https://doi.org/10.1016/S0079-6611(02)00024-1).
- Sheppard, C. R., et al. (2012), Reefs and islands of the Chagos Archipelago, Indian Ocean: Why it is the world's largest no-take marine protected area, *Aquat. Conserv. Mar. Freshw. Ecosyst.*, *22*(2), 232–261. <https://doi.org/10.1002/aqc.1248>.
- Sprintall, J., A. L. Gordon, A. Koch-Larrouy, T. Lee, J. T. Potemra, K. Pujiana, and S. E. Wijffels (2014), The Indonesian seas and their role in the coupled ocean–climate system, *Nat. Geosci.*, *7*(7), 487–492. <https://doi.org/10.1038/ngeo2188>.

- Srokosz, M. A., J. Robinson, H. McGrain, E. E. Popova, and A. Yool (2015), Could the Madagascar bloom be fertilized by Madagascar iron? *J. Geophys. Res. Oceans*, *120*, 5790–5803. <https://doi.org/10.1002/2015JC011075>.
- Stoner, A. W., M. H. Davis, and C. J. Booker (2012), Abundance and population structure of queen conch inside and outside a marine protected area: Repeat surveys show significant declines, *Mar. Ecol. Prog. Ser.*, *460*, 101–114. <https://doi.org/10.3354/meps09799>.
- Talley, L. D., G. L. Pickard, W. J. Emery, and J. H. Swift (2011), *Descriptive Physical Oceanography: An Introduction*, 6th ed., pp., Elsevier, Oxford, U. K.; Burlington, Vermont and San Diego, Calif.
- The Pew Charitable Trusts (2015), *Pew, National Geographic Applaud Creation of Pitcairn Islands Marine Reserve*, edited by A. Risotto, The Pew Charitable Trusts, London, U. K.
- The Red List (2015), The IUCN Red List of threatened species. Version 2015–4, *Table 6a: Red List Category Summary Country Totals (Animals)*.
- The World Bank (2006), Scaling up marine management: The role of marine protected areas, *Rep. No. 36635*, The Int. Bank for Reconstr. and Dev./The World Bank, Washington, D. C.
- United Nations Environment Programme (2016), *Marine Plastic Debris and Microplastics? Global Lessons and Research to Inspire Action and Guide Policy Change*, United Nations Environ. Program., Nairobi, Kenya.
- Wace, N. (1995), Ocean litter stranded on Australian coast, in *State of the Marine Environment Report for Australia: Technical Annex 2 – Pollution*, edited by L. P. Zann and D. Sutton, Great Barrier Reef Mar. Park Auth., Townsville, Australia.
- Watson, R., and D. Pauly (2001), Systematic distortions in world fisheries catch trends, *Nature*, *414*(6863), 534–536. <https://doi.org/10.1038/35107050>.
- Wernberg, T., B. D. Russell, P. J. Moore, S. D. Ling, D. A. Smale, A. Campbell, M. A. Coleman, P. D. Steinberg, G. A. Kendrick, and S. D. Connell (2011), Impacts of climate change in a global hotspot for temperate marine biodiversity and ocean warming, *J. Exp. Mar. Biol. Ecol.*, *400*(1–2), 7–16. <https://doi.org/10.1016/j.jembe.2011.02.021>.
- Wright, S. L., R. C. Thompson, and T. S. Galloway (2013), The physical impacts of microplastics on marine organisms: A review, *Environ. Pollut.*, *178*, 483–492. <https://doi.org/10.1016/j.envpol.2013.02.031>.
- Wu, L., et al. (2012), Enhanced warming over the global subtropical western boundary currents, *Nat. Clim. Change*, *2*(3), 161–166. <https://doi.org/10.1038/nclimate1353>.
- Wyrtki, K. (1973), An equatorial jet in the Indian Ocean, *Science*, *181*, 262–264. <https://doi.org/10.1126/science.181.4096.262>.
- Yang, H., G. Lohmann, W. Wei, M. Dima, M. Ionita, and J. Liu (2016), Intensification and poleward shift of subtropical western boundary currents in a warming climate, *J. Geophys. Res. Oceans*, *121*, 4928–4945. <https://doi.org/10.1002/2015jc011513>.